POLITECNICO DI TORINO
Repository ISTITUZIONALE

Acute Cardiovascular Response to Gravity Changes: A Multiscale Mathematical Model for Microgravity and Hypergravity Applications

Original
Acute Cardiovascular Response to Gravity Changes: A Multiscale Mathematical Model for Microgravity and Hypergravity Applications / Tripoli, Francesco; Ridolfi, Luca; Scarsoglio, Stefania. - 2:(2024), pp. 1106-1117. (2024 IAF/IAA Space Life Sciences Symposium at the 75th International Astronautical Congress, IAC 2024 Milano (Ita) 14-18 October 2024) [10.52202/078355-0132].

Availability:
This version is available at: 11583/3000499 since: 2025-05-29T14:49:39Z

Publisher:
International Astronautical Federation, IAF

Published
DOI:10.52202/078355-0132

Terms of use:

This article is made available under terms and conditions as specified in the corresponding bibliographic description in the repository

Publisher copyright

(Article begins on next page)

13 May 2026

Copyright ©2024 by the International Astronautical Federation (IAF). All rights reserved.

IAC-24,A1,IP,120,x83272

Acute cardiovascular response to gravity changes: a multiscale mathematical model for microgravity and hypergravity applications

F. Tripoli[a]*, L. Ridolfi[b], S. Scarsoglio[a],

[a] *Department of Mechanical and Aerospace Engineering, Politecnico di Torino, Corso Duca degli Abruzzi 24, Turin, 10129, Italy*
[b] *Department of Environmental, Land and Infrastructure Engineering, Politecnico di Torino, Corso Duca degli Abruzzi 24, Turin, 10129, Italy*
* Corresponding Author, francesco.tripoli@polito.it

Abstract

In recent years, several studies revealed that long-term human spaceflights induce many cardiovascular alterations (from blood volume decrease to cardiac atrophy), which seriously threaten the health of the astronauts. Among all the hazards of the space environment, continuous exposure to gravity changes (from micro- to hyper-gravity) plays a crucial role in the cardiovascular response to such a hostile environment. However, hemodynamic characterization is still incomplete, and no definitive data are available to date. In this context, numerical modeling provides a useful tool for evaluating cardiovascular and cerebral adaptation to spaceflight environments.

To investigate the acute cardiovascular response in standing posture to gravity changes (from 0g to 2.5g), we propose a multiscale 0D-1D model combining a closed-loop central-systemic cardiovascular 0D-1D model with two 0D cerebrovascular and ocular models. The overall model is equipped with short-term regulation mechanisms (baroreflex, cardiopulmonary, cerebral and CO_2 reactivity), and explicitly accounts for the action of venous collapse, and gravity and posture changes.

Our analysis reveals that: (i) as gravity increases from 0g to 2.5g a worsening of several cardiac and mechano-energetic parameters is observed: heart rate (HR) increases from approximately 65 bpm to 110 bpm, while stroke volume (SV), ejection fraction (EF) and cardiac output (CO) decrease respectively by about -47%, -7% and -9%. Furthermore, these parameters show a non-linear behaviour with g; (ii) gravitational acceleration greatly affects both pressures and flow rates, in terms of mean and pulsatile values, along the arterial tree; (iii) in microgravity (0g-1g), ICP and IOP rise due to a head-ward fluid shift caused by the absence of gravitational force, while in hypergravity (1g-2.5g) they exhibit a significant reduction. Conversely, cerebral blood flow (CBF) remains relatively stable within the range of 0g-1g, but decreases rapidly with higher g values, suggesting an inability of cerebral autoregulation to maintain an adequate CBF.

In conclusion, in the short-term, the 0g condition is less demanding, yet it exposes the cerebral-ocular circulation to heightened intracranial and intraocular pressure. Conversely, hypergravity conditions induce strong orthostatic stress, decreasing both SV and cerebral perfusion.

Keywords: Computational hemodynamics, microgravity, hypergravity, space medicine

Nomenclature

($\overline{CBF}$) Mean values of cerebral blood flow
($\overline{ICP}$) Mean values of intracranial pressure
($\overline{IOP}$) Mean values of intraocular pressure
($\overline{P}$) Mean values of arterial pressure
($\overline{Q}$) Mean values of arterial flow rate
(ΔCBF) Pulsatile values cerebral blood flow
(ΔICP) Pulsatile values of intracranial pressure
(ΔIOP) Pulsatile values of intraocular pressure
(ΔP) Pulsatile values of arterial pressure
(ΔQ) Pulsatile values of arterial flow rate

Acronyms/Abbreviations

(*CBF*) Cerebral blood flow
(*CO*) Cardiac output
(ECA) External carotid artery
(*EF*) Ejection Fraction
(g) Gravity acceleration
(G-LOC) G-induced loss of consciousness
(*HR*) Heart rate
(ICA) Internal carotid artery
(*ICP*) Intracranial pressure
(*IOP*) Intraocular pressure
($P_{a,eye}$) Arterial pressure at eye level
(SANS) Spaceflight Associated Neuro-ocular Syndrome
(*SV*) Stroke volume

1. Introduction

Despite the significant interest in human space exploration, human adaptation to the space environment

Copyright ©2024 by the International Astronautical Federation (IAF). All rights reserved.

is still an argument of many unanswered questions. In recent years, the cardiovascular system's response to gravitational acceleration changes has been studied extensively [1-6], yet many physiological mechanisms remain unclear and need to be clarified to ensure the health and safety of astronauts [7-8]. During spaceflights, the human body undergoes different levels of gravitational force, ranging from weightlessness (microgravity condition) to increased gravitational stress experienced during launch or landing maneuvers (hypergravity condition). Both conditions exert considerable stress on the cardiovascular system: (i) microgravity induces a fluid shift in the headward directions and, during long-term spaceflights, the absence of gravity is the main cause of blood volume reduction, cardiac atrophy and reduced exercise capacity [9-10]; (ii) hypergravity entails significant orthostatic stress and induces a fluid shift from the intrathoracic compartment to the legs [1], leading to reduced venous return. Moreover, cerebral arterial pressure decreases due to the gravity-dependent hydrostatic term, and this can lead to reduced cerebral perfusion when pressure falls below the cerebral autoregulation range [1, 11]. This reduction in CBF can result in syncope and G-LOC [11-12].

The mimicking of gravity changes can be achieved in an affordable and cost-effective controlled environment by exploiting ground-based analogs, such as bed-rest studies, dry immersions, parabolic flights and centrifuges. In bed-rest studies, the gravity vector is aligned along the antero-posterior axis, while in dry immersions, gravitational force is neutralized by the immersion of the body into a liquid. However, both bed-rest tests and immersions are not able to fully replicate the microgravity environment, as they introduce horizontal forces and hydrostatic pressure gradients [13-14]. Parabolic flight is able to reproduce actual microgravity and hypergravity conditions, yet these conditions are sustained only for a few seconds [15-16]. Human centrifuges are able to simulate the hypergravity conditions by producing a centrifugal force acting along the longitudinal axis of the body. This force is dependent on both the rotation rate and the distance from the axis of rotation. Consequently, the centrifuge generates a gravity gradient along the head-to-feet axis.

Given the above difficulties in reproducing the actual microgravity and hypergravity conditions, mathematical modeling represents a promising alternative for studying the cardiovascular response to gravity changes. This approach offers the ability to study hemodynamic parameters that are difficult to measure directly – such as *ICP* and *IOP* – and to investigate physiological mechanisms. Mathematical models have already demonstrated their usefulness and reliability in various areas of hemodynamics, allowing the cardiovascular system to be studied with different levels of detail (from lumped-parameters models to 3D reconstructed models) [17-21]. E.g., multiscale models, have been exploited to investigate the cardiovascular system under different circumstances – such as cardiac arrhythmias [22-23], head-up and head-down tilt tests [24-26], parabolic flights [27], human centrifuges [28] and long-term spaceflights [29].

In this work, we aim to investigate the short-term cardiovascular response in standing posture to gravity changes – from 0g to 2.5g – through multiscale mathematical modeling. This response is primarily governed by short-term regulation mechanisms – such as arterial baroreflex, cardiopulmonary reflex and cerebral autoregulation – and occurs within few seconds following the application of an external stimulus. For this purpose, we exploited a validated 0D-1D model [26] composed of a 0D-1D model of the systemic circulation, a 0D model of the cerebrovascular circulation, and a 0D ocular model. The model was here improved by including the venous collapse of the neck veins.

This approach enables us to describe the hemodynamics, including flow rates and pressures, at different locations along the arterial tree, and to investigate the main cardiac (*HR*, *SV*, *CO*, *EF*) and cerebral-ocular (*ICP*, *IOP*, *CBF*, $P_{a,eye}$) quantities, highlighting non-linear behaviours as gravitational acceleration changes.

2. Material and methods

This section provides an overview of the multiscale mathematical model adopted in this work, highlighting its main features and architecture, and outlining the improvements introduced in this study. Comprehensive details of the model, including the governing equations, the numerical methods and the parameter settings can be found in previous works [26, 30].

The proposed multiscale 0D-1D cardiovascular-cerebral-ocular model combines a closed-loop central-systemic cardiovascular 0D-1D model with two 0D cerebrovascular and ocular models.

2.1 Central-systemic cardiovascular 0D-1D model

The closed-loop central-systemic cardiovascular model includes the 1D description of the arterial tree and the 0D representation of the peripheral microcirculation, the venous return, and the cardio-pulmonary circulation.

The 1D representation of the arterial tree is composed of 63 main arteries. Blood motion through 1D arteries follows the axisymmetric form of Navier-Stokes equations for mass and momentum balance, where blood is modeled as an incompressible and Newtonian fluid. Gravitational acceleration is directly accounted for in the governing equations, considering the orientation of the arteries relative to both the frontal axis and the horizontal plane. To close the mathematical model, a constitutive non-linear law – linking arterial blood pressure and

Copyright ©2024 by the International Astronautical Federation (IAF). All rights reserved.

vessel cross-sectional area and accounting for vessels' viscoelastic properties – is considered [31].

The 0D description of the model consists of several RLC models representing the arteriolar, capillary, venular and venous compartments. In particular, each 1D terminal artery is linked to a 0D arteriolar lumped-parameters model. The downstream circulation of these 0D arteriolar models is organized into five body regions: head, arms, upper abdomen, lower abdomen and legs. Each of these regions is described by the series of three 0D analog electric models representing capillary, venular and venous compartments, respectively. To complete the venous return to the heart, three 0D compartments representing the superior, inferior and abdominal venae cavae are included.

The cardio-pulmonary circulation comprises the description of the four cardiac chambers along with the representation of the pulmonary circulation. Cardiac valves are depicted as non-ideal diodes, whereas the contractile capacity of the atria and ventricles is modeled via time-varying elastances, linking the transmural pressure with the volume of the chamber. The pulmonary circulation is described through an arterial and a venous RC compartment. To account for the action of the intrathoracic pressure, a relationship linking the intrathoracic pressure with gravitational acceleration and body position is used.

To describe the short-term regulation mechanisms, the model is equipped with both a baroreflex and a cardio-pulmonary model.

2.2 0D cerebrovascular-ocular model

The 0D model of cerebrovascular circulation is directly coupled with the internal carotid and vertebral arteries of the central-systemic cardiovascular model. The model describes the main cerebral features through a combination of resistances and compliances. The large cerebral arteries and the circle of Willis are included, and the downstream circulation is organized in six distinct vascular districts, mimicking the pial arterial-arteriolar circulation. Each district is connected through a distal cortical anastomosis. To maintain an adequate cerebral blood flow, the compliances and resistances of the six vascular beds are controlled by the cerebral autoregulation mechanism. The post-capillary circulation is described as a unique pathway from cerebral capillaries to dural venous sinuses. The processes of cerebrospinal fluid formation and absorption are modeled through resistive components, while the intracranial pressure is computed by applying the mass preservation and assuming a non-linear pressure-volume relationship for the craniospinal system. The cerebral venous outflow is coupled with the superior vena compartment.

The 0D model of the eye includes six compartments and the behaviour of the intraocular pressure and ocular globe volume is regulated by two governing equations. The ocular model is linked to the central-systemic cardiovascular model at the level of internal carotid arteries, while the ocular outflow is directly connected to the outlet venous district of the 0D cerebral model.

2.3 Collapse of the neck veins

Recent studies suggested that venous collapse of internal jugular veins due to postural or gravity changes affects the intracranial pressure. In particular, Homlund et al [32] proposed a new model where the collapse of the internal jugular veins hydrostatically disconnects the intracranial and extracranial venous system, reducing the hydrostatic effects in the cerebrospinal fluid system. To account for these mechanisms, two main improvements are introduced compared to our previous model: (i) a non-linear pressure-volume relationship is introduced to model the collapsibility of the neck veins; (ii) the hydrostatic term in the ICP governing equation changes during the collapse of the neck veins.

In our model, internal jugular veins are included in the superior vena cava compartment, which directly connects the cerebral model with the cardio-pulmonary system. The non-linear pressure-volume relationship employed in this work is an adaptation of the equation proposed by Lu et al [33] to describe the collapse of the vena cava. This relationship is expressed as follows:

$$P_{svc} = \frac{(V_{svc} - V_{svc}^{un})}{C_{svc}} + P_{off}, \qquad if\ V_{svc} \geq V_{svc}^{un} \tag{1}$$

$$P_{svc} = D_2 + K_2 \cdot e^{\left(\frac{V_{svc}}{V_{svc}^{min}}\right)}, \qquad if\ V_{svc} < V_{svc}^{un} \tag{2}$$

where V_{svc} and P_{svc} denote the volume and transmural pressure of the superior vena cava, V_{svc}^{un} is the unstressed volume, V_{svc}^{min} is the minimum volume. The parameters P_{off} and K_2 were chosen to ensure that both the function and its first derivative exhibit continuity at V_{svc}^{un}, while the value of V_{svc}^{min} was adjusted according to the unstressed volume of the superior vena cava compartment in order to maintain the same proportion with the values defined by Lu et al [33] (see Tab. 1).

Furthermore, two non-linear relationships for both the resistance and inertance are included:

$$R_{svc} = R_{svc}^{0} \left(\frac{V_{svc}^{0}}{V_{svc} - V_{svc}^{min}}\right)^2 \tag{3}$$

$$L_{svc} = L_{svc}^{0} \left(\frac{V_{svc}^{0}}{V_{svc} - V_{svc}^{min}}\right) \tag{4}$$

where R_{svc}^{0}, L_{svc}^{0} and V_{svc}^{0} correspond to the initial values at $t = 0$.

To address the hydrostatic decoupling that occurs during venous collapse, only the hydrostatic gradient corresponding to the fluid column extending from dural venous sinuses to the most cranial point of jugular collapse is considered. Hence, the dural venous sinus pressure applied to the outflow of the 0D cerebral model and the hydrostatic term in the ICP governing equation are computed as:

$$P_{dvs} = P_{svc} - \rho g \left(\frac{L_H}{3} + \frac{L_{svc}}{2}\right), \qquad if\ V_{svc} \geq V_{svc}^{un} \tag{5}$$

Copyright ©2024 by the International Astronautical Federation (IAF). All rights reserved.

$$P_{dvs} = P_{svc} - \rho g\left(\frac{L_H}{3}\right), \qquad if\ V_{svc} < V_{svc}^{un} \quad (6)$$

$$ICP^h = \rho g\left(\frac{L_H}{3} + \frac{L_{svc}}{2}\right)\sin\alpha, \qquad if\ V_{svc} \geq V_{svc}^{un} \quad (7)$$

$$ICP^h = \rho g\left(\frac{L_H}{3}\right)\sin\alpha\,, \qquad if\ V_{svc} < V_{svc}^{un} \quad (8)$$

where P_{svc} is superior vena cava pressure, ρg is blood specific weight, α is the tilt angle, L_H is the head compartment extension and L_{svc} is the superior vena cava compartment extension.

Table 1. Parameter values for venous collapse model

Parameters	Values
C_{svc} (ml/mmHg)	5
D_2 (mmHg)	0
K_2 (mmHg)	0.4113
L_H (cm)	15
L_{svc} (cm)	17
L_{svc}^0 (mmHg s^2/ml)	0.000005
P_{off} (mmHg)	5.586
R_{svc}^0 (mmHg s/ml)	0.00055
V_{svc}^0 (ml)	145.72
V_{svc}^{min} (ml)	27.93
V_{svc}^{un} (ml)	72.86

3. Results

The proposed model was used to investigate the acute cardiovascular response in standing posture to gravity changes. The results are organized by initially showing the response of some of the most significant cardiac parameters – *HR*, *SV*, *CO* and *EF* – and the behaviours of pressures and flow rates along the 1D arterial tree. Then, the response of the main cerebral and ocular quantities – *ICP*, *IOP*, *CBF*, $P_{a,eye}$ – is described.

Fig. 1 shows the behaviour of the investigated cardiac parameters within the gravity range of [0*g*-2.5*g*]. The *HR* exhibits a non-linear trend in the microgravity range [0*g*-1*g*], decreasing from 77 bpm to 65 bpm (-15.8%) as gravity diminishes from 1*g* to 0*g* and reaching a minimum value of 64 bpm at 0.2*g*. Conversely, the *HR* increases linearly from 77 bpm to 113 bpm (+46.5%) as gravitational acceleration grows from 1*g* to 2.5*g*. The *SV* rises in the microgravity range (+26.8% from 1*g* to 0*g*), while it decreases from 64.4 ml to 42.9 ml (-33.4%) within the hypergravity range [1*g*-2.5*g*]. This reduction is triggered by a fluid shift from the upper body to the lower body that occurs when gravitational force increases. Due to the short-term regulation mechanisms, the *CO* remains relatively stable throughout the gravity range. In fact, as gravity decreases from 1*g* to 0*g*, the *CO* rises from 5 ml/s to 5.3 ml/s (+6.8%), while the *CO* decreases up to 4.8 ml/s at 2.5*g* (-2.4%). The *EF* which measures the heart's pumping capability, behaves similarly to the *CO*. In particular, the *EF* rises from 58% to 61% as gravity decreases from 1*g* to 0*g*, while it decreases up to 56.5% at 2.5*g*.

An overview of arterial pressures in seven different districts along the 1D arterial tree in relation to gravitational acceleration is depicted in Fig. 2. For each arterial district the pressure's behaviour is investigated in terms of mean and pulsatile values ($\overline{P}$ and ΔP). Arterial intravascular pressures are strictly influenced by a gravity-dependent hydrostatic component, which becomes increasingly relevant as both the distance from the heart and the gravitational acceleration rise. Starting from the ascending aorta (see Fig. 2a), a slight increase from 92.7 mmHg at 0*g* to 97 mmHg at 1*g* (+4.6%) in mean arterial pressure is observed. This increase results from the inotropic effect on both ventricles and the control of peripheral vascular resistance – both short-term mechanisms of the autonomic nervous system – which prevent a drop in systemic mean arterial pressure. As gravity increases, $\overline{P}$ is nearly constant throughout the remaining gravity range. Conversely, ΔP experiences great variations, growing from 42 mmHg at 1*g* to 51 mmHg at 0g (+21% from 1*g* to 0*g*), and decreasing up to 28.9 mmHg at 2.5*g* (-31.4%). This behaviour is induced by the strict correlation between ΔP at the central aortic level and *SV* [4]. In fact, as previously mentioned, *SV* increases within the microgravity range, thus leading to heightened pulsatility of the arterial systemic pressure. On the contrary, *SV* decreases in hypergravity, resulting in reduced ΔP.

Moving in the headward direction, the mean arterial pressure in the ECA (see Fig. 2b) is greatly affected by the gravity-dependent hydrostatic component of the pressure. In fact, $\overline{P}$ grows from 86.8 mmHg at 1*g* to 94.8 mmHg at 0*g* (+9.3%) and decreases up to 65.6 mmHg at 2.5g (-32.1%). Conversely to the pressure behaviour observed in the ascending aorta, ΔP in the ECA is nearly constant throughout the range [0*g*-2.5*g*]. The pressure in the thoracic aorta (see Fig. 2c) exhibits similar behaviour to the pressure in the ascending aorta, as both sites are approximately at the same height. In particular, $\overline{P}$ shows a non-monotonic trend, increasing from 94.5 mmHg to 95.7 mmHg as gravity grows from 0*g* to 1*g* and reaching a maximum value of 97.2 mmHg at 0.5*g*. In the hypergravity range $\overline{P}$ decreases up to 88.5 mmHg at 2.5*g* (-8.1% from 1*g* to 2.5*g*). In addition, ΔP decreases from 57 mmHg at 0*g* to 39 mmHg at 2.5*g* (-31.5%).

As the distance from the heart increases along the caudal direction, the mean arterial pressure begins to follow a monotonic trend and increases with gravitational acceleration. This increase is proportional to the distance of each anatomical site from the heart. Hence, at the tibial level (see Fig. 2g) the hydrostatic term results in a more than threefold increase in mean arterial pressure, growing from 90 mmHg at 0*g* to 275 mmHg at 2.5*g* (+205%). Similarly, at the femoral (see Fig. 2f), iliac (see Fig. 2e) and abdominal (see Fig. 2d) arteries, the mean arterial pressure grows by +111%, 71%, and 41%, respectively.

Copyright ©2024 by the International Astronautical Federation (IAF). All rights reserved.

Pulsatile values of the pressure increase along the arterial tree due to wave propagation [34]. As a result, at 0g ΔP rises from 61.8 mmHg in the abdominal aorta to 102.9 mmHg in the anterior tibial artery. Despite this increase, the variation in ΔP over the range of [0g-2.5g] partially restores along the caudal direction. Specifically, ΔP decreases by -33.8% in the abdominal aorta, and by -27.3%, -24.5% and -25% in the iliac, femoral and tibial arteries, respectively.

Fig. 3 illustrates the variations in flow rate mean and pulsatile values ($\overline{Q}$ and ΔQ) across the same sites of Fig. 2 along the 1D arterial tree under varying gravitational acceleration. In the first tract of the ascending aorta (see Fig. 3a), the mean arterial flow rate mirrors the behaviour of *CO*, exhibiting the same non-monotonic trend. As gravity decreases from 1g to 0g, $\overline{Q}$ increases from 76.2 ml/s to 82.7 ml/s (+8.5%). In the interval of [0.5g-1.5g], $\overline{Q}$ is nearly constant. Beyond this range, the mean flow rate decreases, reaching 71.6 ml/s at 2.5g (-6%). Analysis of ΔQ reveals that the minimum values of flow rate do not display a clear trend in response to changes in gravitational acceleration. Conversely, the flow rate maximum values decrease with increasing gravity, resulting in a -17.6% reduction in ΔQ within the gravity range of [0g-2.5g].

In the external carotid artery (see Fig. 3b), the mean flow rate decreases gradually as gravitational acceleration increases due to the associated pressure drop induced by elevated gravitational force. In fact, the ECA primarily supplies blood to peripheral and extracranial structures of the head. These structures are not directly involved in the cerebral autoregulation mechanism. Hence, $\overline{Q}$ decreases monotonically from 1.8 ml/s to 0.98 ml/s, resulting in a -46.4% drop as gravity increases from 0g to 2.5g. As previously observed with ΔP, ΔQ is relatively stable throughout the gravity spectrum and, interestingly, exhibits a slight increase from 17.3 ml/s at 0g to 19.84 at 2.5g.

The thoracic aorta (see Fig. 3c) shows a decrease in both $\overline{Q}$ and ΔQ as gravity increases, following a similar trend to that observed in the ascending aorta. In particular, $\overline{Q}$ increases by +14.1% as g decreases from 1g to 0g, whereas it declines by -7.3% at 2.5g. Similarly, the main factor contributing to the decrease in ΔQ – specifically a reduction of -23.6% as gravitational acceleration increases from 0g to 2.5g – is the decline in maximum flow rate values.

The abdominal aorta (see Fig. 3d) and the common iliac artery (see Fig. 3e) display similar behaviours: both mean flow rates show an initial decline – from 21.3 ml/s to 19.49 ml/s in the abdominal aorta and from 6.2 ml/s to 5.6 ml/s in the common iliac artery – within the range of [0g-0.5g]. Following this decline, both $\overline{Q}$ exhibit a modest recovery, reaching their maximum in the proximity of 1.5g. Beyond this value, both arteries experience another reduction in the mean flow rate values, decreasing to 19.2 ml/s and 5.5 ml/s at 2.5g, respectively. Both arteries show a reduction of ΔQ – by -35.6% in the abdominal aorta and by -31.1% in the common iliac artery – as g changes from 0g to 2.5g.

The femoral artery (see Fig. 3f) and the anterior tibial artery (see Fig. 3g), located further along the caudal direction, show a monotonic increase in mean flow rates as gravitational acceleration grows. In particular, $\overline{Q}$ in the femoral artery rises from 2.1 ml/s at 0g to 4 ml/s at 2.5g, while an increase from 1.1 ml/s at 0g to 2.4 ml/s at 2.5g in the anterior tibial artery is observed. In addition, both arteries display a reduction in ΔQ as gravity increases. This decline in pulsatility is associated with a simultaneous rise in the minimum flow rate values and a decrease in the maximum flow rate values. Specifically, from 0g to 2.5g, ΔQ decreases by -39.4% in the femoral artery and by -40.4% in the anterior tibial artery.

Fig. 4 illustrates the key parameters describing the ocular and cerebral hemodynamics. In particular, mean and pulsatile values of the arterial pressure in the ICA, the *CBF*, the *ICP* and the *IOP* are depicted. As previously described, the gravity-dependent hydrostatic component of the pressure greatly impacts cerebral arterial pressure. The mean arterial pressure in the ICA (see Fig 4a) grows when entering the microgravity range (+34.6% from 1g to 0g). As expected, in the hypergravity range $\overline{P}$ decreases abruptly by –63.3% at 2.5 with respect to the 1g baseline condition, thus greatly reducing the cerebral perfusion pressure. As a consequence of the reduction of the pulse pressure at the central aortic level, ΔP monotonically declines as gravity increases, diminishing by -60.2% at 2.5g. Due to cerebral autoregulation mechanisms, $\overline{CBF}$ (see Fig 4b) remains relatively stable within the range of [0g-1g], with variations limited to -10% up to approximately 2g. Beyond this threshold, cerebral autoregulation loses the capability of maintaining adequate perfusion, leading to a reduction of -17% at 2.5g. Due to the reduced cerebral arterial pulse pressure and the heightened inertia of the deep cerebral circulation – which further amplifies (in microgravity) or damps (in hypergravity) the increased or reduced pulsatility at central aortic level [35-36] – ΔCBF increases by up to +75.4% at 0g with respect to the 1g condition, while it decreases by -78.5% at 2.5g.

Fig. 4c describes the response of *ICP* to gravity changes. In particular, as gravity decreases from 1g to 0g, $\overline{ICP}$ rises from 0.9 mmHg to 10.1 mmHg due to the headward fluid shift occurring in the microgravity environment. In addition, $\overline{ICP}$ exhibits non-linear trend, showing a distinct slope variation at 0.5g. This behaviour is associated with the venous collapse mechanism that occurs in the neck veins. In fact, the collapse of the internal jugular veins hydrostatically decouples the intracranial and extracranial venous regions, reducing the

Copyright ©2024 by the International Astronautical Federation (IAF). All rights reserved.

hydrostatic column and the hydrostatic pressure term [32]. This mechanism plays a fundamental role in preventing an excessive reduction in *ICP* during hypergravity conditions. Furthermore, a decrease in ΔICP from 1.7 mmHg at $0g$ to 1.1 mmHg at $2.5g$ is observed.

Fig. 4d depicts the *IOP* non-linear trend in response to gravitational acceleration changes. In particular, $\overline{IOP}$ shows a convex shape due to the reduction of the rate of $\overline{IOP}$ decrease. Therefore, the greatest variations of *IOP* occur within the microgravity range – where an increase from 13.7 mmHg to 18.6 mmHg (+35.8% from $1g$ to $0g$) is observed – due to the microgravity-induced cephalad fluid shift. Conversely, at $2.5g$ $\overline{IOP}$ decreases by -21.9% compared to the normal gravity condition. In addition, ΔIOP monotonically decreases from 5.2 mmHg to 2 mmHg as gravity rises from $0g$ to $2.5g$.

4. Discussion

In this work, we investigated the acute cardiovascular and cerebral responses in standing posture to gravity changes, ranging from $0g$ (microgravity) to $2.5g$ (hypergravity), by coupling a 0D-1D central systemic cardiovascular model with two 0D cerebral and ocular circulation models. The results show that variations in gravitational acceleration elicit a number of hemodynamic alterations: from an increase in *SV*, *ICP* and *IOP* and a decrease in *HR* during microgravity to a reduction in venous return, cerebral perfusion pressure and cerebral blood flow in hypergravity, together with alterations in arterial pressures and flow rates along the arterial tree.

Gravity-induced blood volume redistribution – from the lower to the upper body during microgravity and from the central to the lower regions during hypergravity – triggers the response of the autonomic nervous system (baroreceptor and cardiopulmonary reflexes), which exerts chronotropic/inotropic effects on the heart and regulates both peripheral vascular resistance and venous tone. Consequently, during high gravitational stress, the *HR* grows to mitigate the effects of a reduced venous return and to compensate for the decrease in the *SV*, maintaining a near constant *CO*. Our results align with those observed in centrifuges studies [37-39], which investigated the effects of hypergravity and gravity acceleration changes on the cardiovascular and cerebral systems.

The analysis of the arterial pressure highlights the influence of the gravity-dependent hydrostatic term on mean arterial pressure and pulsatility. The significant increase of arterial pressure in the lower extremities during hypergravity elicits an increased blood flow at both femoral and tibial levels. In addition, the concurrent pressure reduction in the upper regions of the body induces a decline in cerebral perfusion pressure. To maintain an adequate *CBF* the cerebral autoregulation elicits a vasodilatory response, reducing the vascular resistance. However, this mechanism is able to regulate *CBF* for cerebral perfusion pressures within the range [50 mmHg-150 mmHg] [11, 40]. Below this range, *CBF* rapidly decreases leading to the development of presyncope after a reduction in *CBF* of 50-60% [11]. Our results show a decrease of almost 20% in *CBF* as gravity increases from $0g$ to $2.5g$, with most of the variation taking place beyond $2g$, suggesting an inability of cerebral autoregulation to maintain the *CBF* at higher g values.

Due to the microgravity-induced fluid shift in the cranial direction both *ICP* and *IOP* grow with respect to the normal gravity condition. In fact, our model predicts an increase in $\overline{ICP}$ from 0.9 mmHg to 10.1 mmHg, whereas $\overline{IOP}$ rises from 13.7 mmHg to 18.6 mmHg. These results are coherent with *ICP* values measured during tilt test studies and *IOP* measurements in the microgravity environment [32, 41, 42, 43]. Notably, *ICP* grows more than *IOP* within the microgravity range, thus leading to a variation in their interaction. In recent years, several studies suggested that this relationship between *ICP* and *IOP* might be involved in the onset of SANS [44-46]. In particular, the higher increase in *ICP* leads to an alteration of the translaminar pressure – defined as the difference between *IOP* and *ICP* – that is the differential pressure across the lamina cribrosa, potentially leading to optic nerve diseases and eye remodeling [46-47]. Conversely, due to the large reduction in *ICP* occurring in the hypergravity range, the translaminar pressure increases. Recalling that the collapse of the internal jugular veins might play a crucial role in avoiding an excessive decrease in *ICP* [32], this two-phase behaviour of the intracranial pressure might prevent abnormally elevated differential pressure across the lamina cribrosa under increased gravitational acceleration.

The computational approach presented in this study has certain limitations. Specifically, long-term regulation mechanisms, transcapillary fluid exchange with the interstitium, cerebral reactivity to different levels of CO_2 and the action of the muscular system are neglected.

5. Conclusions

In conclusion, our multiscale mathematical model highlights the great impact of gravitational acceleration on the human cardio- and cerebrovascular systems and is able to predict quantities that are difficult to measure directly – such as pressures and flow rates waveforms along the arterial tree, from the cerebral regions to lower limbs, as well as *IOP*, *ICP* and *CBF* beat-averaged and pulsatile behaviour – giving interesting insights in physiological hemodynamic alterations that occur in the micro- and hypergravity environments. The proposed mathematical modeling represents a promising tool to investigate the cardiovascular responses to both micro-

Copyright ©2024 by the International Astronautical Federation (IAF). All rights reserved.

and hypergravity and can support the development and optimization of new spaceflight countermeasures.

Acknowledgments

This study was carried out within the I-2022-05387 "Optimizing countermeasures against cardiovascular deconditioning and cerebral hemodynamics changes in long-term human spaceflights" project, which was selected via the Open Space Innovation Platform (https://ideas.esa.int) as a Co-Sponsored Research Agreement and carried out under the Discovery programme of, and funded by, the European Space Agency (contract number: 4000141523). This manuscript reflects only the authors' views and opinions and the European Space Agency cannot be considered responsible for them.

References

[1] Blomqvist, C. G., & Stone, H. L. (1991). Cardiovascular adjustments to gravitational stress. NASA. Lyndon B. Johnson Space Center, Spacelab Life Sciences 1: Reprints of Background Life Sciences Publications.

[2] Buckey, J. C. (2006). Space physiology. Oxford University Press, USA.

[3] Clément, G. (2011). Fundamentals of space medicine (Vol. 23). Springer science & business media.

[4] Hall, J. E., & Hall, M. E. (2020). Guyton and Hall Textbook of Medical Physiology E-Book: Guyton and Hall Textbook of Medical Physiology E-Book. Elsevier Health Sciences.

[5] Aubert, A. E., Beckers, F., & Verheyden, B. (2005). Cardiovascular function and basics of physiology in microgravity. Acta cardiologica, 60(2), 129-151.

[6] Grigoriev, A. I., Kotovskaya, A. R., & Fomina, G. A. (2011). The human cardiovascular system during space flight. Acta Astronautica, 68(9-10), 1495-1500.

[7] Blaber, E., Marçal, H., & Burns, B. P. (2010). Bioastronautics: the influence of microgravity on astronaut health. Astrobiology, 10(5), 463-473.

[8] Seidler, R. D., Stern, C., Basner, M., Stahn, A. C., Wuyts, F. L., & Zu Eulenburg, P. (2022). Future research directions to identify risks and mitigation strategies for neurostructural, ocular, and behavioral changes induced by human spaceflight: A NASA-ESA expert group consensus report. Frontiers in Neural Circuits, 16, 876789.

[9] Norsk, P., Asmar, A., Damgaard, M., & Christensen, N. J. (2015). Fluid shifts, vasodilatation and ambulatory blood pressure reduction during long duration spaceflight. The Journal of physiology, 593(3), 573-584.

[10] Zhu, H., Wang, H., & Liu, Z. (2015). Effects of real and simulated weightlessness on the cardiac and peripheral vascular functions of humans: A review. International Journal of Occupational Medicine and Environmental Health, 28(5), 793-802.

[11] Folino, A. F. (2007). Cerebral autoregulation and syncope. Progress in cardiovascular diseases, 50(1), 49-80.

[12] Shender, B. S., Forster, E. M., Hrebien, L., Ryoo, H. C., & Cammarota, J. P. (2003). Acceleration-induced near-loss of consciousness: the "A-LOC" syndrome. Aviation, space, and environmental medicine, 74(10), 1021-1028.

[13] Saveko, A., Bekreneva, M., Ponomarev, I., Zelenskaya, I., Riabova, A., Shigueva, T., ... & Tomilovskaya, E. (2023). Impact of different ground-based microgravity models on human sensorimotor system. Frontiers in Physiology, 14, 1085545.

[14] Watenpaugh, D. E. (2016). Analogs of microgravity: head-down tilt and water immersion. Journal of Applied Physiology, 120(8), 904-914.

[15] Shelhamer, M. (2016). Parabolic flight as a spaceflight analog. Journal of applied physiology, 120(12), 1442-1448.

[16] Karmali, F., & Shelhamer, M. (2008). The dynamics of parabolic flight: flight characteristics and passenger percepts. Acta astronautica, 63(5-6), 594-602.

[17] Mynard, J. P., & Smolich, J. J. (2015). One-dimensional haemodynamic modeling and wave dynamics in the entire adult circulation. Annals of biomedical engineering, 43, 1443-1460.

[18] Blanco, P. J., & Feijóo, R. A. (2013). A dimensionally-heterogeneous closed-loop model for the cardiovascular system and its applications. Medical Engineering & Physics, 35(5), 652-667..

[19] Liang, F., Takagi, S., Himeno, R., & Liu, H. (2009). Multi-scale modeling of the human cardiovascular system with applications to aortic valvular and arterial stenoses. Medical & biological engineering & computing, 47, 743-755.

[20] Marsden, A. L., & Esmaily-Moghadam, M. (2015). Multiscale modeling of cardiovascular flows for clinical decision support. Applied Mechanics Reviews, 67(3), 030804.

[21] Scarsoglio, S., Saglietto, A., Tripoli, F., Zwanenburg, J. J., Biessels, G. J., De Ferrari, G. M., ... & Ridolfi, L. (2022). Cerebral hemodynamics during atrial fibrillation: Computational fluid dynamics analysis of lenticulostriate arteries using 7 T high-resolution magnetic resonance imaging. Physics of Fluids, 34(12).

[22] Anselmino, M., Scarsoglio, S., Saglietto, A., Gaita, F., & Ridolfi, L. (2016). Transient cerebral hypoperfusion and hypertensive events during atrial fibrillation: a plausible mechanism for cognitive impairment. Scientific reports, 6(1), 28635.

[23] Saglietto, A., Scarsoglio, S., Ridolfi, L., Gaita, F., & Anselmino, M. (2019). Higher ventricular rate during

Copyright ©2024 by the International Astronautical Federation (IAF). All rights reserved.

atrial fibrillation relates to increased cerebral hypoperfusions and hypertensive events. Scientific reports, 9(1), 3779.

[24] Heldt, T., Shim, E. B., Kamm, R. D., & Mark, R. G. (2002). Computational modeling of cardiovascular response to orthostatic stress. Journal of applied physiology, 92(3), 1239-1254.

[25] Whittle, R. S., & Diaz-Artiles, A. (2021). Modeling individual differences in cardiovascular response to gravitational stress using a sensitivity analysis. Journal of Applied Physiology, 130(6), 1983-2001..

[26] Fois, M., Diaz-Artiles, A., Zaman, S. Y., Ridolfi, L., & Scarsoglio, S. (2024). Linking cerebral hemodynamics and ocular microgravity-induced alterations through an in silico-in vivo head-down tilt framework. npj Microgravity, 10(1), 22.

[27] Fois, M., Ridolfi, L., & Scarsoglio, S. (2022). In silico study of the posture-dependent cardiovascular performance during parabolic flights. Acta Astronautica, 200, 435-447.

[28] Diaz-Artiles, A., Heldt, T., & Young, L. R. (2019). Computational model of cardiovascular response to centrifugation and lower body cycling exercise. Journal of Applied Physiology, 127(5), 1453-1468.

[29] Gallo, C., Ridolfi, L., & Scarsoglio, S. (2020). Cardiovascular deconditioning during long-term spaceflight through multiscale modeling. npj Microgravity, 6(1), 27.

[30] Fois, M., Maule, S. V., Giudici, M., Valente, M., Ridolfi, L., & Scarsoglio, S. (2022). Cardiovascular response to posture changes: multiscale modeling and in vivo validation during head-up tilt. Frontiers in Physiology, 13, 826989.

[31] Guala, A., Camporeale, C., Tosello, F., Canuto, C., & Ridolfi, L. (2015). Modelling and subject-specific validation of the heart-arterial tree system. Annals of biomedical engineering, 43, 222-237.

[32] Holmlund, P., Eklund, A., Koskinen, L. O., Johansson, E., Sundström, N., Malm, J., & Qvarlander, S. (2018). Venous collapse regulates intracranial pressure in upright body positions. American Journal of Physiology-Regulatory, Integrative and Comparative Physiology, 314(3), R377-R385.

[33] Lu, K., Clark Jr, J. W., Ghorbel, F. H., Ware, D. L., & Bidani, A. (2001). A human cardiopulmonary system model applied to the analysis of the Valsalva maneuver. American Journal of Physiology-Heart and Circulatory Physiology, 281(6), H2661-H2679.

[34] Van de Vosse, F. N., & Stergiopulos, N. (2011). Pulse wave propagation in the arterial tree. Annual Review of Fluid Mechanics, 43(1), 467-499.

[35] Scarsoglio, S., Fois, M., & Ridolfi, L. (2023). Increased hemodynamic pulsatility in the cerebral microcirculation during parabolic flight-induced microgravity: A computational investigation. Acta Astronautica, 211, 344-352.

[36] Scarsoglio, S., Saglietto, A., Anselmino, M., Gaita, F., & Ridolfi, L. (2017). Alteration of cerebrovascular haemodynamic patterns due to atrial fibrillation: an in silico investigation. Journal of The Royal Society Interface, 14(129), 20170180.

[37] Fontolliet, T., Pichot, V., Antonutto, G., Bonjour, J., Capelli, C., Tam, E., ... & Ferretti, G. (2015). Effects of gravitational acceleration on cardiovascular autonomic control in resting humans. European journal of applied physiology, 115, 1417-1427.

[38] Ueda, K., Ogawa, Y., Yanagida, R., Aoki, K., & Iwasaki, K. I. (2015). Dose-effect relationship between mild levels of hypergravity and autonomic circulatory regulation. Aerospace medicine and human performance, 86(6), 535-540.

[39] Ogawa, Y., Yanagida, R., Ueda, K., Aoki, K., & Iwasaki, K. I. (2016). The relationship between widespread changes in gravity and cerebral blood flow. Environmental health and preventive medicine, 21, 186-192.

[40] Blaber, A. P., Zuj, K. A., & Goswami, N. (2013). Cerebrovascular autoregulation: lessons learned from spaceflight research. European journal of applied physiology, 113, 1909-1917.

[41] Lawley, J. S., Petersen, L. G., Howden, E. J., Sarma, S., Cornwell, W. K., Zhang, R., ... & Levine, B. D. (2017). Effect of gravity and microgravity on intracranial pressure. The Journal of physiology, 595(6), 2115-2127.

[42] Anderson, A. P., Swan, J. G., Phillips, S. D., Knaus, D. A., Kattamis, N. T., Toutain-Kidd, C. M., ... & Buckey, J. C. (2016). Acute effects of changes to the gravitational vector on the eye. Journal of Applied Physiology, 120(8), 939-946.

[43] Mader, C. T. H., Gibson, C. R., Caputo, M., Hunter, N., Taylor, G., Charles, J., & Meehan, R. T. (1993). Intraocular pressure and retinal vascular changes during transient exposure to microgravity. American journal of ophthalmology, 115(3), 347-350.

[44] Zhang, L. F., & Hargens, A. R. (2018). Spaceflight-induced intracranial hypertension and visual impairment: pathophysiology and countermeasures. Physiological reviews, 98(1), 59-87.

[45] Marshall-Goebel, K., Mulder, E., Bershad, E., Laing, C., Eklund, A., Malm, J., ... & Rittweger, J. (2017). Intracranial and intraocular pressure during various degrees of head-down tilt. Aerospace medicine and human performance, 88(1), 10-16.

[46] Berdahl, J. P., Yu, D. Y., & Morgan, W. H. (2012). The translaminar pressure gradient in sustained zero gravity, idiopathic intracranial hypertension, and glaucoma. *Medical hypotheses*, *79*(6), 719-724.

[47] Taibbi, G., Cromwell, R. L., Kapoor, K. G., Godley, B. F., & Vizzeri, G. (2013). The effect of

Copyright ©2024 by the International Astronautical Federation (IAF). All rights reserved.

microgravity on ocular structures and visual function:
a review. Survey of ophthalmology, 58(2), 155-163.

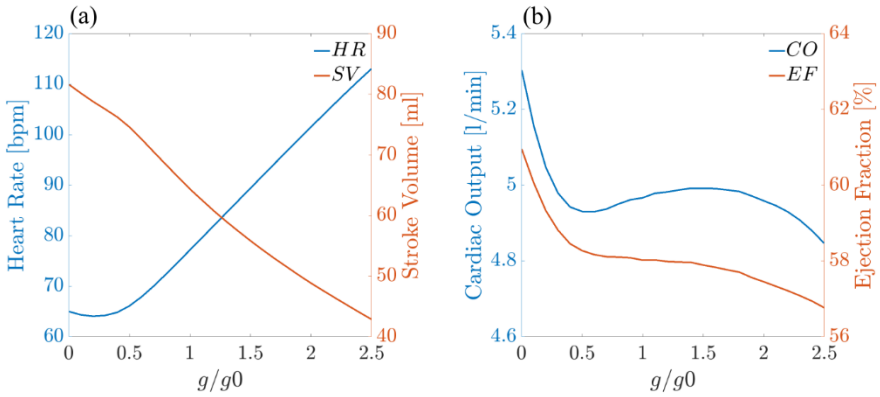

Fig. 1. Cardiac parameters in relation to gravitational acceleration: a) *HR* and *SV*; b) *CO* and *EF*.

Copyright ©2024 by the International Astronautical Federation (IAF). All rights reserved.

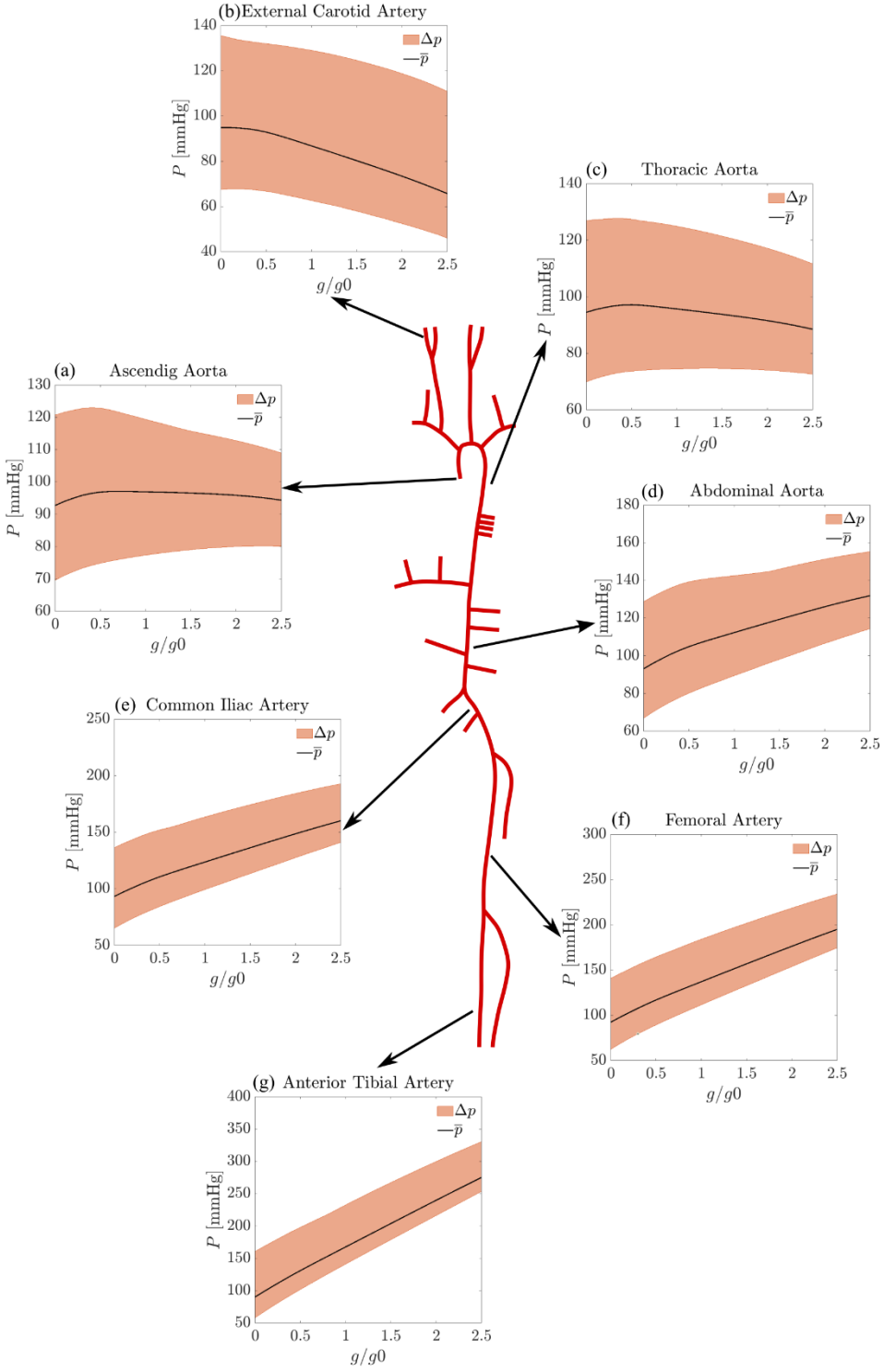

Fig. 2. Pressure signals along the arterial tree during gravity change. In each panel, the black line indicates the mean value $\overline{P}$.

Copyright ©2024 by the International Astronautical Federation (IAF). All rights reserved.

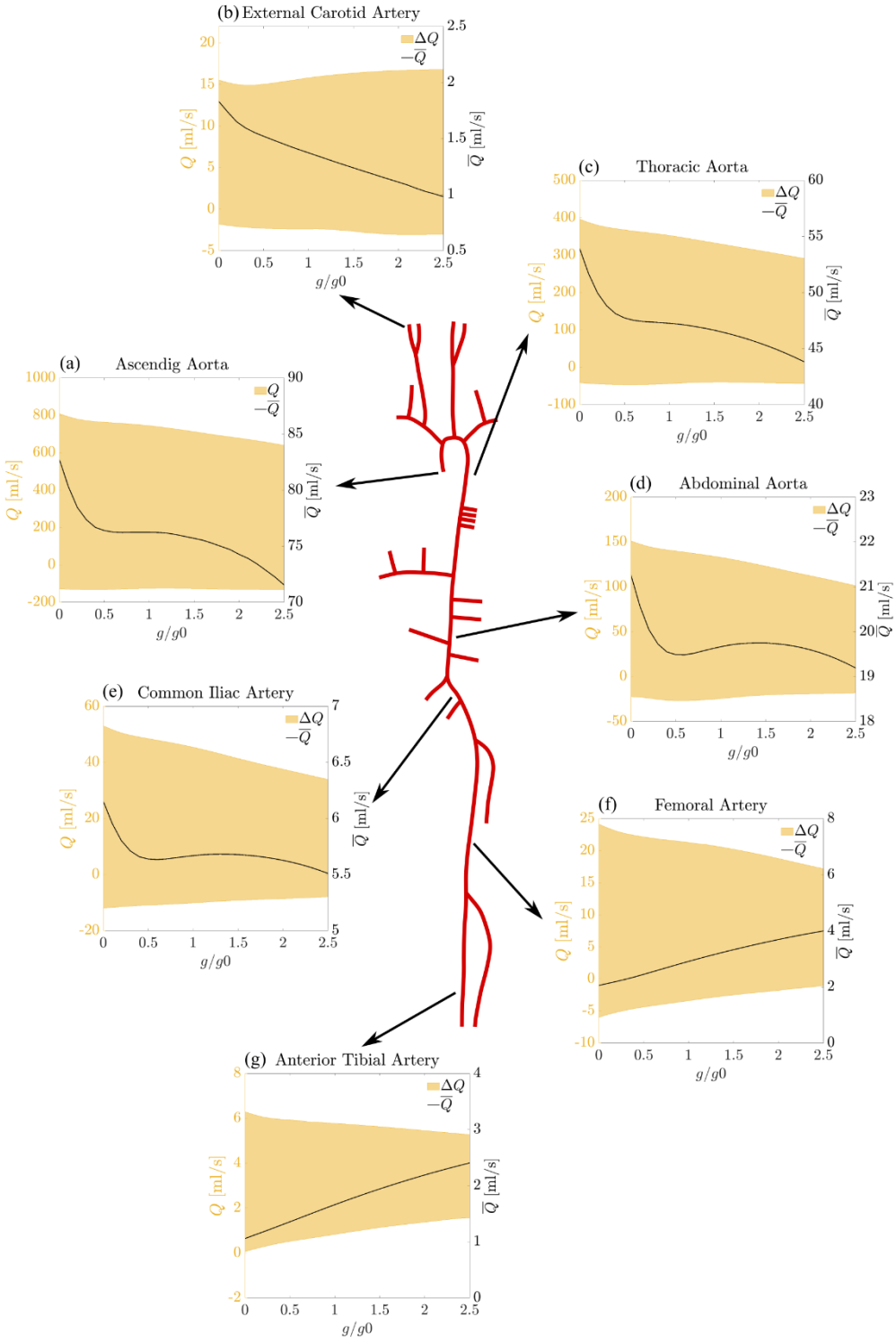

Fig. 3. Flow rate signals along the arterial tree during gravity change. In each panel, the black line indicates the mean value $\overline{Q}$.

Copyright ©2024 by the International Astronautical Federation (IAF). All rights reserved.

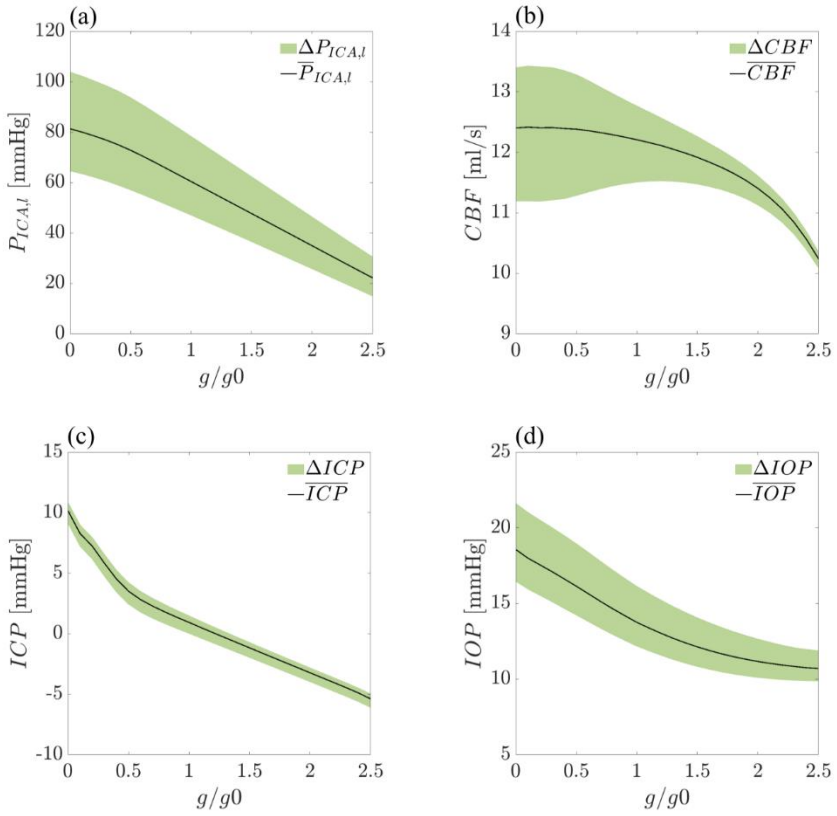

Fig. 4. Cerebral and ocular parameters in relation to gravitational acceleration.